SUPPLEMENTARY MATERIALS AND METHODS

Fly stocks and genetics

Mutants used included *slmb*^{1}, *slmb*^{2}, *slmb*^{8}, *dlg*$^{40-2}$, *Roc1a*^{G1}, *AP-2sigma* and *yki*^{B5} (described in FlyBase). Transgenes included *tub>slmb-myc* (Ko et al., 2002), *UAS-Ci*$^{M1-4}$ (Chen et al., 1999), *UAS-Arm*^{S10} (Pai et al., 1997), *UAS-Plk4*^{SBM} (Rogers et al., 2009), *UAS-CapH2*^{SBM} (Buster et al., 2013), *UAS-Par1*^{T408A} (Lee et al., 2012), *UAS-aPKC*$^{CAAX-DN}$ (Sotillos et al., 2004) and *UAS-aPKC*$^{\delta N}$ (Betschinger et al., 2003) driven by *MS1096-GAL4*, as well as *hs-Wls-V5* and *UAS-Wls-V5* (Belenkaya et al., 2008). Entirely mutant wing discs were generated using *UbxFLP/FM7; cl FRT82B/TM6B* and entirely mutant eye discs were generated using *eyFLP cl GMRhid FRT82B/TM6B*. MARCM clones in the eye and neuroblast were generated with *eyFLP* and *hsFLP* stocks, respectively. Follicle cell clones were generated as described (Lu and Bilder, 2005).

Immunohistochemistry

The following primary antibodies were used: mouse anti-Mmp1 (1/100), mouse anti-Arm (N27A1, 1/100), mouse anti-Dlg (4F3, 1/100), mouse anti-Coracle (1/100), mouse anti-FasIII (7G10, 1/20), mouse anti-Notch^{ECD} (C458.2H, 1/50), mouse anti-Lamin (1/100), rat anti-Elav (9F8A9, 1/50) (all from Developmental Studies Hybridoma Bank, see references therein), rat anti-Crb (1/750; U. Tepass, E. Knust), guinea pig anti-Cad87E (1/1000; U. Tepass), guinea pig anti-Scrib (1/200), rabbit anti-PKCζ (sc-216, Santa Cruz Biotechnology, 1/200), rabbit anti-Miranda (1/500), mouse anti-Prospero (1/100). TRITC-phalloidin was used to visualize F-actin (1/400, Sigma) and either TO-PRO-3 (1/400) or DAPI (1/3000) was used to visualize DNA. Secondary antibodies were from Molecular Probes.

Supplementary references

Belenkaya, T. Y., Wu, Y., Tang, X., Zhou, B., Cheng, L., Sharma, Y. V., Yan, D., Selva, E. M. and Lin, X. (2008). The retromer complex influences Wnt secretion by recycling wntless from endosomes to the trans-Golgi network. *Dev Cell* **14**, 120–131.

Betschinger, J., Mechtler, K. and Knoblich, J. A. (2003). The Par complex directs asymmetric cell division by phosphorylating the cytoskeletal protein Lgl. *Nature* **422**, 326–330.

Buster, D. W., Daniel, S. G., Nguyen, H. Q., Windler, S. L., Skwarek, L. C., Peterson, M., Roberts, M., Meserve, J. H., Hartl, T., Klebba, J. E., et al. (2013). SCFSlimb ubiquitin ligase suppresses condensin II-mediated nuclear reorganization by degrading Cap-H2. *J. Cell Biol.* **201**, 49–63.

Chen, Y., Cardinaux, J. R., Goodman, R. H. and Smolik, S. M. (1999). Mutants of cubitus interruptus that are independent of PKA regulation are independent of hedgehog signaling. *Development* **126**, 3607–3616.

Ko, H. W., Jiang, J. and Edery, I. (2002). Role for Slimb in the degradation of Drosophila Period protein phosphorylated by Doubletime. *Nature* **420**, 673–678.

Lee, S., Wang, J.-W., Yu, W. and Lu, B. (2012). Phospho-dependent ubiquitination and degradation of PAR-1 regulates synaptic morphology and tau-mediated Aβ toxicity in Drosophila. *Nature Communications* **3**, 1312–12.

Lu, H. and Bilder, D. (2005). Endocytic control of epithelial polarity and proliferation in Drosophila. *Nat. Cell Biol.* **7**, 1232–1239.

Pai, L. M., Orsulic, S., Bejsovec, A. and Peifer, M. (1997). Negative regulation of Armadillo, a Wingless effector in Drosophila. *Development* **124**, 2255–2266.

Rogers, G. C., Rusan, N. M., Roberts, D. M., Peifer, M. and Rogers, S. L. (2009). The SCF Slimb ubiquitin ligase regulates Plk4/Sak levels to block centriole reduplication. *J. Cell Biol.* **184**, 225–239.

Sotillos, S., Diaz-Meco, M. T., Caminero, E., Moscat, J. and Campuzano, S. (2004). DaPKC-dependent phosphorylation of Crumbs is required for epithelial cell polarity in Drosophila. *J. Cell Biol.* **166**, 549–557.

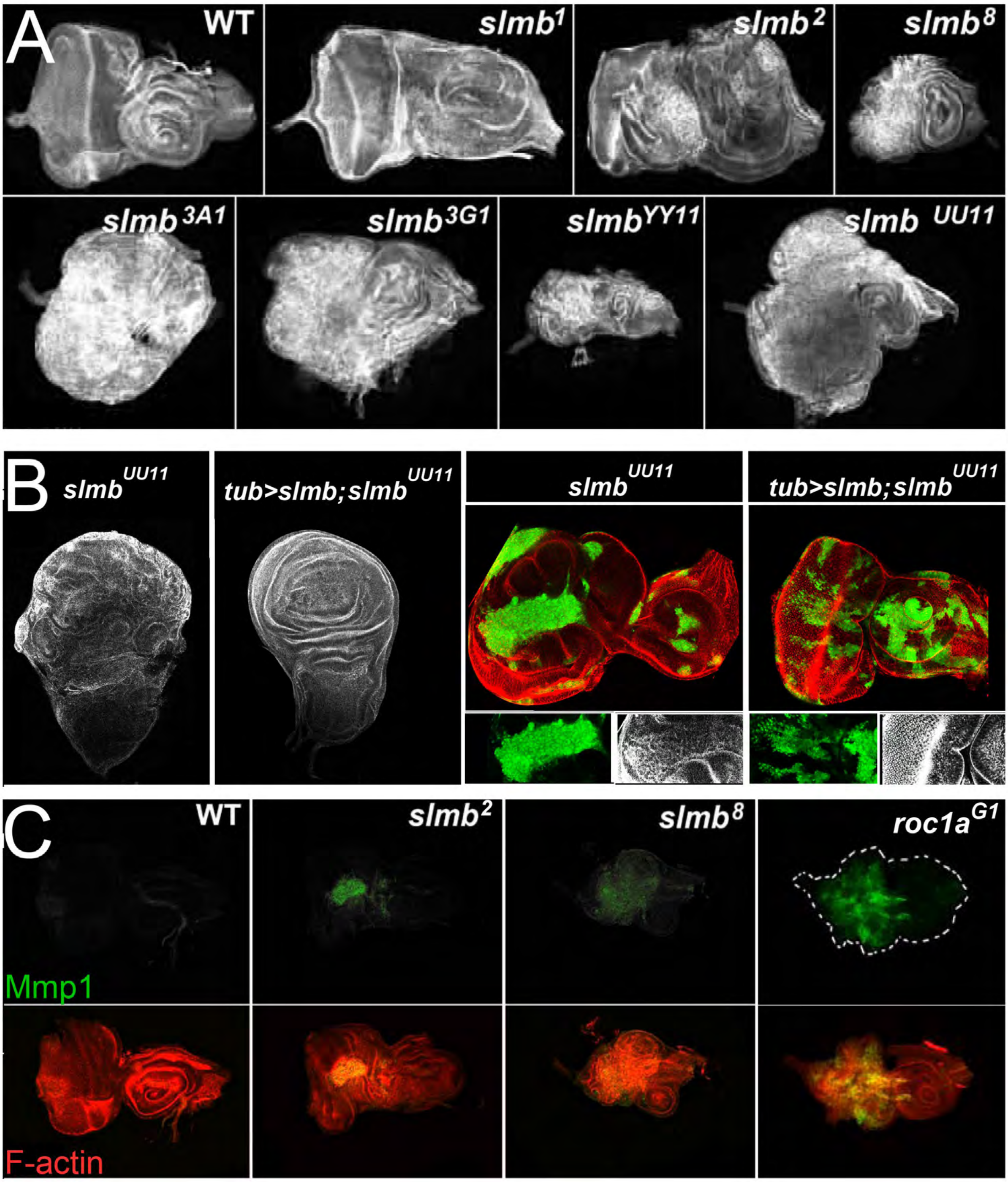

Supplementary Figure 1. Analysis of *slmb* allelic series. (**A**) Phalloidin staining of *slmb* mutant eye discs demonstrates that strong alleles show the most severe neoplastic transformation. (**B**) A *slmb* transgene rescues the neoplastic phenotypes of *UU11* in predominantly mutant wing discs and GFP-marked eye disc mosaics. (**C**) Discs derived from the deletion allele *slmb*^{8} and null mutation in the SCF core component *roc1a* also display hallmarks of neoplasia, including disrupted F-Actin and upregulation of Mmp1.

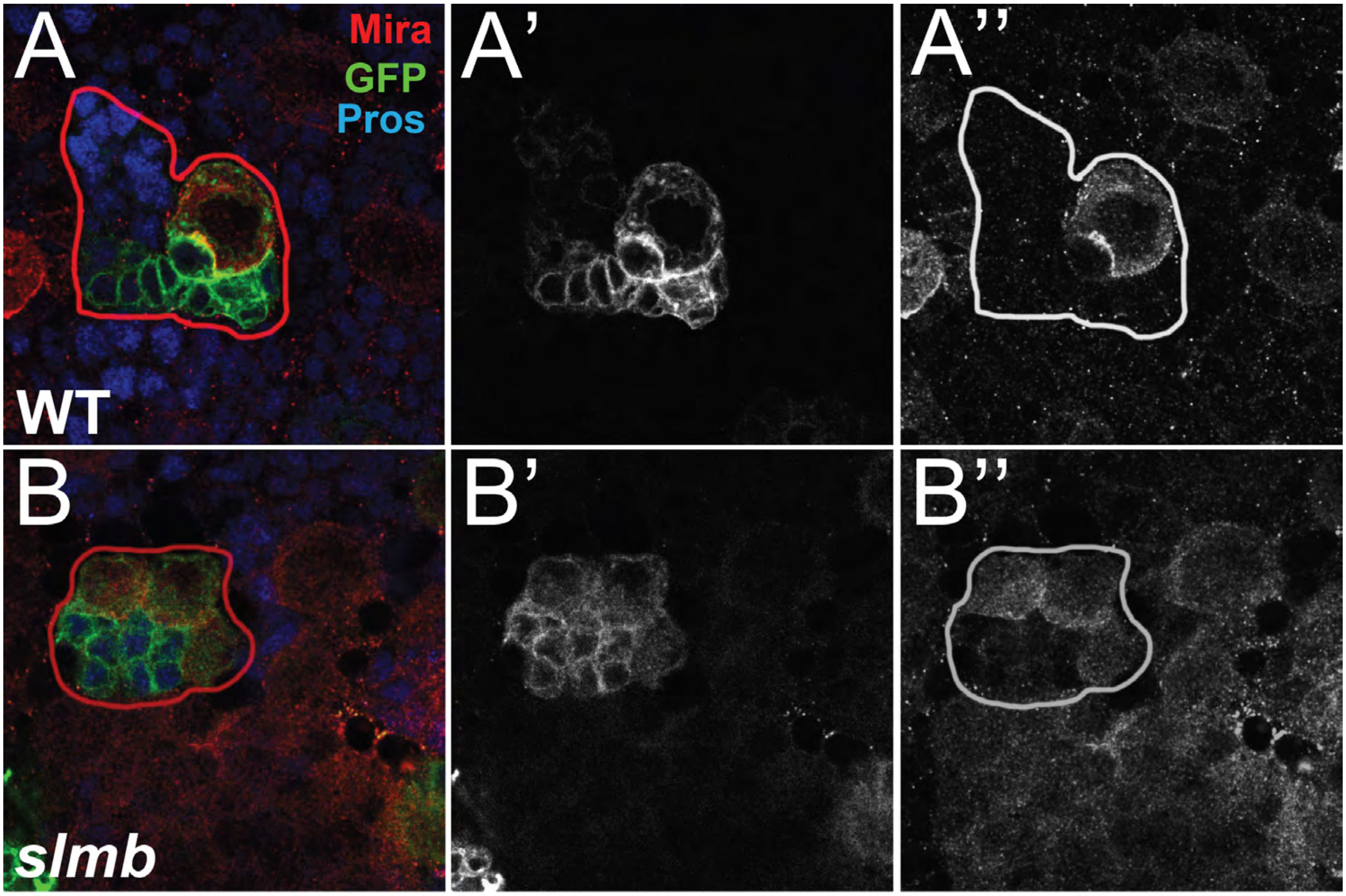

Supplementary Figure 2. Effect of loss of *slmb* in neuroblasts. (**A, B**) GFP marks clones generated using the MARCM system. Larval type I neuroblasts divide asymmetrically to produce a new Miranda-positive neuroblast (red) and a smaller ganglion mother cell that will differentiate into a neuron or glia (Prospero positive, blue). *slmb* mutant neuroblasts display defects in asymmetric cell division, with a fraction of clones containing multiple Miranda positive neuroblast-like cells.

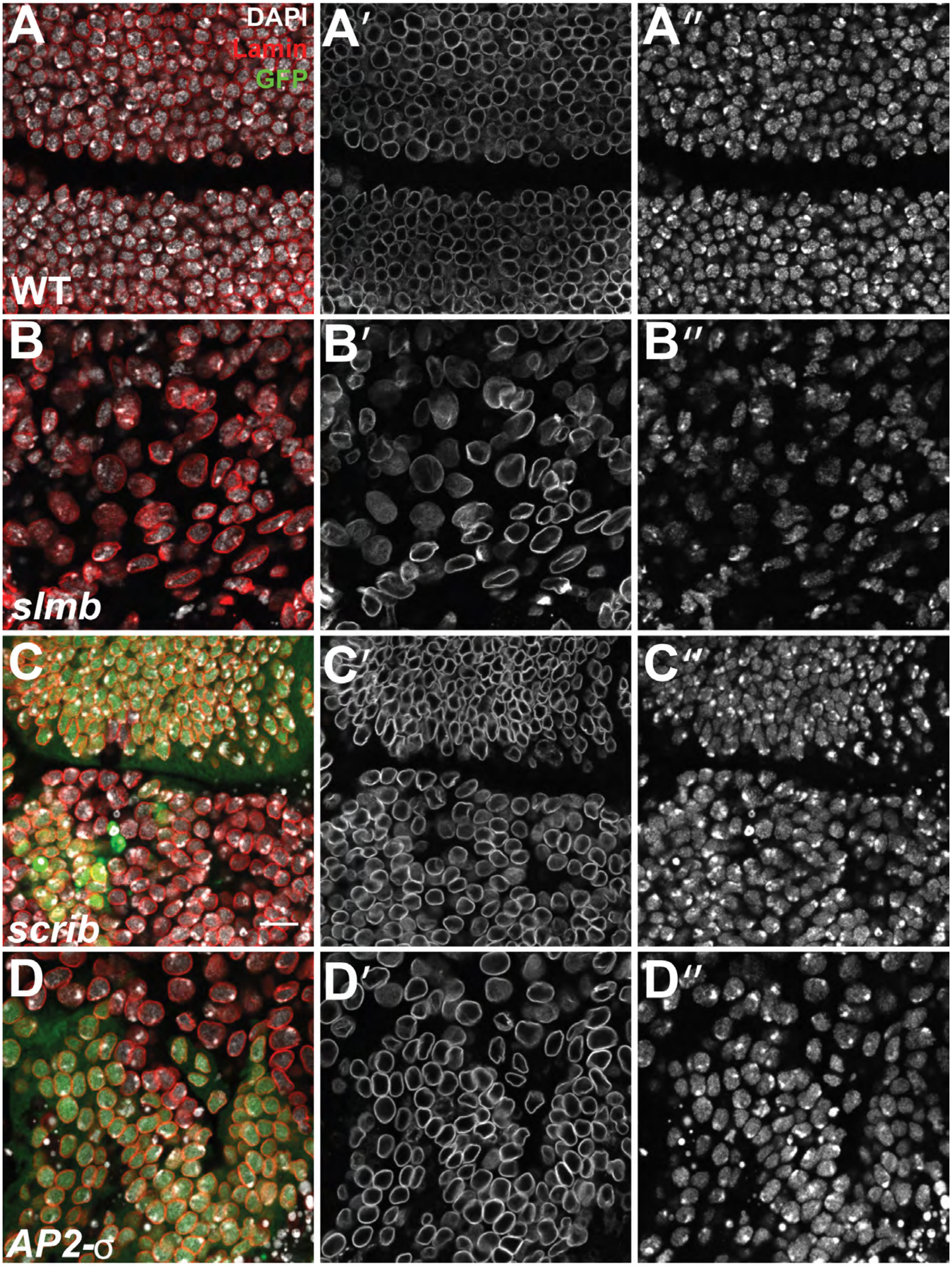

Supplementary Figure 3. Junctional scaffold and endocytic class tumor suppressors do not regulate Slmb activity. (**A, B**) Cells mutant for strong *slmb* alleles show chromosome condensation defects leading to a swollen nuclear lamina, reflecting misregulation of Condensin components. (**C,D**) In contrast, *scrib* and *AP2-sigma* mutant cells have WT nuclei and lamina size. Presence of GFP marks mutant cells. Scale, 10 mm.

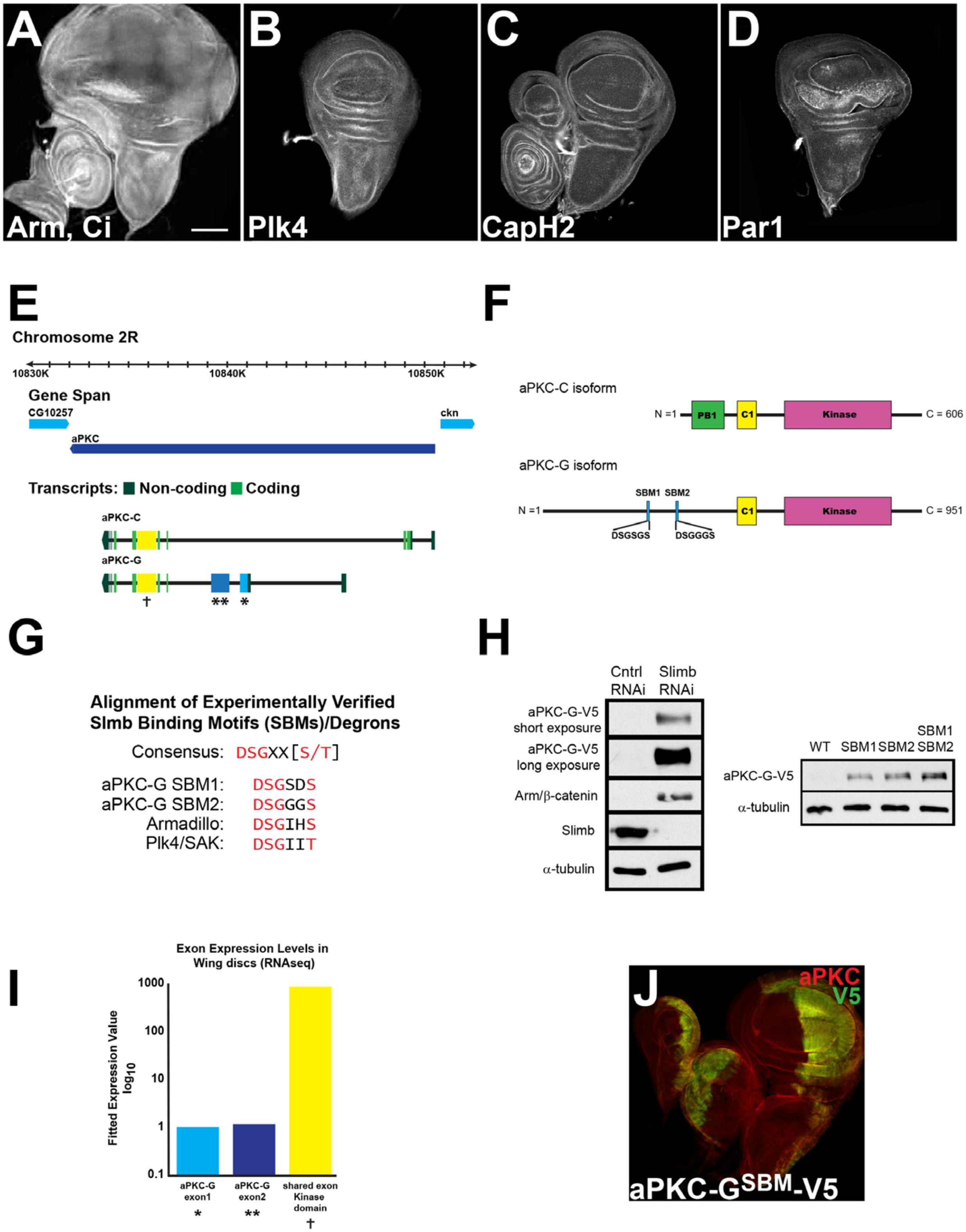

Supplementary Figure 4. Misregulation of known substrates cannot account for the *slmb* phenotype. (**A-D**) Over-expression of stabilized versions of known Slmb substrates throughout the presumptive wing pouch and notum using *MS-1096GAL4* does not phenocopy loss of *slmb*. (**E, F**) Gene and protein models comparing a common aPKC isoform C with the G isoform containing two Slmb binding motifs (SBM). (**G**) Alignment of aPKC-G SBMs with experimentally validated SBM degrons from other Slmb targets. (**H**) Western blots demonstrating that RNAi mediated knockdown of *slmb* in S2 cells results in stabilization of the aPKC-G isoform, as does mutation of the SBMs. (**I**) RNAseq data from third instar wing discs comparing levels of the unique aPKC-G exons with an exon encoding the shared Kinase domain; values shown are derived from RPKM. (**J**) Overexpression of a stabilized version of aPKC-G in the posterior domain of the wing disc (*en>GFP*, green) does not affect polarity or growth.